

AD-A074 761

HARRY DIAMOND LABS ADELPHI MD

F/G 9/5

CHARACTERISTICS OF OROTRON OSCILLATION AND AMPLIFICATION. 1. PO--ETC(U)

JUL 79 R P LEAVITT

UNCLASSIFIED

HDL-TR-1899

NL

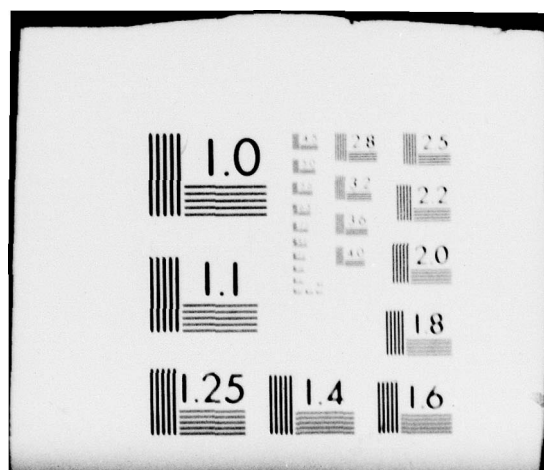
| OF |

AD  
A074761

11



END  
DATE  
FILMED  
11-79  
DDC



AD A 074761

UNCLASSIFIED

SECURITY CLASSIFICATION OF THIS PAGE (When Data Entered)

REPORT DOCUMENTATION PAGE		READ INSTRUCTIONS BEFORE COMPLETING FORM
1. REPORT NUMBER 14 HDL-TR-1899	2. GOVT ACCESSION NO.	3. RECIPIENT'S CATALOG NUMBER 9
4. TITLE (and Subtitle) 6 Characteristics of Orotroon Oscillation and Amplification, 1. Power and Frequency Characteristics.		5. TYPE OF REPORT & PERIOD COVERED Technical Report,
7. AUTHOR(s) 10 Richard P. Leavitt		8. PERFORMING ORG. REPORT NUMBER
9. PERFORMING ORGANIZATION NAME AND ADDRESS Harry Diamond Laboratories 2800 Powder Mill Road Adelphi, MD 20783		10. PROGRAM ELEMENT, PROJECT, TASK AREA & WORK UNIT NUMBERS Prog Elem: 6.11.01.A
11. CONTROLLING OFFICE NAME AND ADDRESS U.S. Army Materiel Development and Readiness Command Alexandria, VA 22333		12. REPORT DATE 11 July 1979
14. MONITORING AGENCY NAME & ADDRESS (if different from Controlling Office) 1218		13. NUMBER OF PAGES 17
15. SECURITY CLASS. (of this report) Unclassified		15a. DECLASSIFICATION/DOWNGRADING SCHEDULE
16. DISTRIBUTION STATEMENT (of this Report) Approved for public release; distribution unlimited.		
17. DISTRIBUTION STATEMENT (of the abstract entered in Block 20, if different from Report)		
18. SUPPLEMENTARY NOTES HDL Project: A10938 DRCMS Code: 611101.91.A001		
19. KEY WORDS (Continue on reverse side if necessary and identify by block number) Near millimeter waves Electron beam radiation devices Smith-Purcell effect Diffraction electronics		
20. ABSTRACT (Continue on reverse side if necessary and identify by block number) Power and frequency characteristics of orotron oscillation and amplification are derived from an equivalent circuit representation of the orotron. Feedback in the orotron (beam bunching) is represented by a negative conductance in parallel with a complex admittance representing the passive open resonator. This system is driven by a current source that represents either noise (Smith-Purcell radiation) in the oscillator mode or an external driver in the amplifier mode. Conditions for excitation of the orotron as an oscillator are derived, and the line width of the output radiation is computed below and above threshold. It is		

DD FORM 1 JAN 73 1473 EDITION OF 1 NOV 65 IS OBSOLETE

UNCLASSIFIED

1 SECURITY CLASSIFICATION OF THIS PAGE (When Data Entered)

163 050

LB

UNCLASSIFIED

SECURITY CLASSIFICATION OF THIS PAGE (When Data Entered)

shown that the orotron acts as a linear amplifier below threshold and the product  $\omega_0(A_p)^{1/2}$  remains constant as a function of beam current, where  $\omega_0$  is the half bandwidth of the device and  $A_p$  is the small-signal power gain. Amplification characteristics are investigated for excitation by a driver with a finite frequency spread.

$\delta\omega(0)$

to 1/2 power

$A(f)$   
?

to 1/2 power

Accession For	
NTIS GNA&I	<input checked="" type="checkbox"/>
DDC TAB	<input type="checkbox"/>
Unannounced	<input type="checkbox"/>
Justification	
By	
Distribution/	
Availability Codes	
Dist	Avail and/or special
A	

UNCLASSIFIED



## CONTENTS

	<u>Page</u>
1. INTRODUCTION .....	5
2. EQUIVALENT CIRCUIT OF OROTRON .....	5
3. OSCILLATION CHARACTERISTICS .....	6
4. AMPLIFICATION CHARACTERISTICS .....	10
4.1 Monochromatic Excitation .....	10
4.2 Excitation by Source of Finite Spectral Width .....	10
5. CONCLUSIONS .....	13
ACKNOWLEDGEMENT .....	13
LITERATURE CITED .....	14
DISTRIBUTION .....	15

## FIGURES

1 Orotron oscillator amplifier, schematic diagram .....	5
2 Orotron equivalent circuit .....	6
3 Power characteristics of orotron oscillation .....	9
4 Line width characteristics of orotron oscillation .....	9
5 Orotron amplifier frequency response: $\delta_p = \delta_a = \Delta$ .....	11
6 Orotron amplifier frequency response: $\delta_p = \delta_a$ , $\Delta = 2\delta_a$ .....	11
7 Orotron amplifier frequency response: $\delta_p = \delta_a$ , $\Delta = 5\delta_a$ .....	12
8 Orotron amplifier frequency response: $\delta_p = \delta_a$ , $\Delta = 0$ .....	12
9 Orotron amplifier frequency response: $\delta_p = 0.4\delta_a$ , $\Delta = 0.5\delta_a$ .....	12
10 Orotron amplifier frequency response: $\delta_p = 0.2\delta_a$ , $\Delta = 0.5\delta_a$ .....	12

## 1. INTRODUCTION

The orotron<sup>1-3</sup> is a new type of electron device for generation and amplification of millimeter wave radiation. The device consists of an electron beam generator and collector and a Fabry-Perot resonator containing one grooved mirror (grating) and one smooth mirror. The principle of operation of the orotron is based on the Smith-Purcell effect.<sup>4</sup>

A previous study\* describes the physical principles of orotron operation and surveys the existing experimental and theoretical literature (mostly from the Soviet Union). To augment the information in that report, quantify its conclusions, and aid in the development of the first operating orotron in the United States (at the Harry Diamond Laboratories), this series of reports will cover theoretical aspects of the orotron problem. This first report covers the power and spectral characteristics of the orotron operating both as an oscillator and as an amplifier.

Section 2 of this report describes the operating principle of the orotron and its relation to a simple equivalent circuit representation. Feedback in the device (via bunching of the electron beam by the rf field in the open resonator) is represented by a negative conductance. Section 3 derives the characteristics of the orotron as an oscillator by using the equivalent circuit of section 2 coupled to a noise source representing the Smith-Purcell radiation. Section 4 describes the characteristics of the orotron as an amplifier for both monochromatic drivers and drivers with a finite spread in frequency.

## 2. EQUIVALENT CIRCUIT OF OROTRON

A diagram of the orotron is shown in figure 1.

<sup>1</sup>F. S. Rusin and G. D. Bogomolov, Soviet Patent No. 195557 (1965).

<sup>2</sup>N. Taguchi and S. Ono, Report of Research Group on Electron Devices (March 1964).

<sup>3</sup>V. P. Shestopalov, *Diffraction Electronics*, Khar'kov (1976) (Trans. U.S. Joint Publication Service, April 1978).

<sup>4</sup>S. J. Smith and E. M. Purcell, *Phys. Rev.*, 92 (1953), 1069.

\*D. F. Wortman and R. P. Leavitt, *Near Millimeter Wave Orotion Research Study*, Harry Diamond Laboratories (October 1978) (draft).

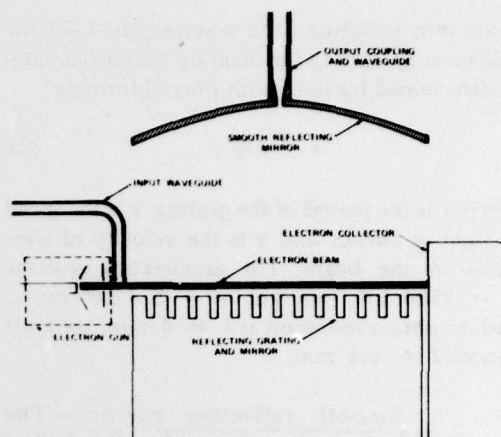


Figure 1. Orotion oscillator amplifier, schematic diagram.

The essential components of the system are as follows:

**Electron gun.**—A uniform sheet beam of electrons is produced by the electron gun. The beam is typically  $0.03 \times 1.0$  cm in cross section and carries a current of 10 to 500 mA. Upon exiting from the gun region, the electrons in the beam have traversed a potential difference of 1000 to 5000 V.

**Electron collector.**—The final resting place for electrons in the beam, the collector, must dissipate several hundreds of watts. The electron collector has no relevance to the rest of this discussion.

**Input waveguide.**—When the orotron is operated as an amplifier, some means must be arranged to provide preliminary modulation of the electron beam by the signal to be amplified. The arrangement shown in figure 1 is one way to provide modulation; electrons passing by the input waveguide are bunched by the incoming rf field, and this bunching leads to an electron density variation at the rf.

**Reflecting grating and mirror.**—One of the mirrors of the Fabry-Perot open resonator contains a reflecting diffraction grating, which converts density fluctuations in the electron

beam into radiation. The wavelength,  $\lambda$ , of the radiation upward in the diagram is approximately determined by the Smith-Purcell formula\*

$$\lambda = l \frac{c}{v}, \quad (1)$$

where  $l$  is the period of the grating,  $c$  is the speed of light in *vacuo*, and  $v$  is the velocity of electrons in the beam. For accelerating voltage  $V = 2500$  kV, we get  $v = 3 \times 10^8$  cm/s, and, to obtain radiation at  $\lambda = 4$  mm, we must choose  $l = 0.4$  mm.

**Smooth reflecting mirror.**—The smooth reflecting mirror forms the other half of the Fabry-Perot resonator and contains the output coupling. The resonator formed by these mirrors is an overmoded cavity having several resonances in the region of interest. By varying the beam accelerating voltage or the mirror spacing, it is possible to excite different resonances; generally, however, for a fixed configuration, only one resonance is excited at a time. Therefore, in what follows, we concern ourselves with a single resonance.

**Output coupling and waveguide.**—Coupling out of the radiation in the orotron is performed by means of a slot in the smooth mirror of the resonator. Dimensions of the slot are generally chosen so that losses due to the slot are comparable to all other losses in the system.

The orotron may be represented by an equivalent circuit,<sup>5</sup> as shown in figure 2. The current source,  $i(\omega)$ , may represent a noise source due to fluctuations in the electron beam current (in the oscillator case) or the modulation in the electron beam due to the driver input (in the amplifier case). The passive open resonator is represented by a complex admittance,

$$Y_0(\omega) = G_0(\omega) + iB_0(\omega). \quad (2)$$

In the vicinity of a resonance at frequency  $\omega_0$ , the admittance may be approximated by

$$Y_0(\omega) \cong G_0 + iB'_0(\omega - \omega_0), \quad (3)$$

where the quantities  $G_0$  and  $B'_0$  are constants (independent of frequency). The output coupling is represented by an additional conductance,  $G_{out}$ , in parallel with  $Y_0$ .

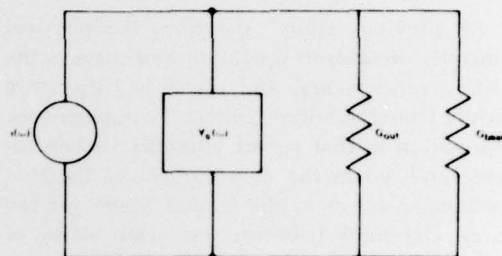


Figure 2. Orotion equivalent circuit.

The important element in the circuit is the negative conductance,  $-G_{beam}$ , which represents the effect of the rf oscillations in the resonator on the electron beam. We can show by the rigorous theory of electron bunching that, with proper synchronism of the electron speed and the phase velocity of rf radiation, the beam bunching leads to radiation into the resonator. The theory predicts linearity of  $G_{beam}$  with electron beam current and also a saturation effect depending on the total rf energy density in the resonator.

The equivalent circuit of figure 2 can be used to derive the power and frequency characteristics of orotron oscillation and amplification. The following sections explore these characteristics.

### 3. OSCILLATION CHARACTERISTICS

The orotron operates as an oscillator when the current source is a low-level noise source (fig. 2). Physically, the noise arises from electron beam current fluctuations, which are transformed into radiation via the Smith-Purcell

\*A. Yariv in *Quantum Electronics*, 2nd ed., John Wiley and Sons, Inc., New York (1975), 300 ff.

\*D. E. Wortman and R. P. Leavitt, *Near Millimeter Wave Orotion Research Study*, Harry Diamond Laboratories (October 1978) (draft).



effect. One may analyze the operation of the oscillator in a first approximation by neglecting this low-level noise.

Consider the equivalent circuit of figure 2 in the absence of the current source,  $i(\omega)$ . Kirchhoff's current equations then require that, if the voltage drop across the circuit is nonzero, the sum of the admittances must vanish. This implies that (eq 3)

$$B_0(\omega - \omega_0) = 0, \quad (4a)$$

$$G_0 + G_{out} - G_{beam} = 0. \quad (4b)$$

Equation (4a) requires that the oscillation be at the resonant frequency,  $\omega_0$ . To interpret equation (4b), recall that the electron beam conductance,  $-G_{beam}$ , is a function of the electron beam current,  $I_0$ , and the total energy density in the resonant cavity,  $U$ . Thus, for a given beam current,  $U$  adjusts itself until equation (4b) is satisfied. Equation (4b) is an implicit equation for  $U$  in terms of  $I_0$ . Since the energy density is directly proportional to the power output,  $P_{out}$ , of the device, one may write  $G_{beam}$  as a function of  $I_0$  and  $P_{out}$ , rather than  $I_0$  and  $U$ .

In an application to a particular example,\*

$$G_{beam} = I_0(\alpha_0 - \alpha_1 P_{out}), \quad (5)$$

where  $\alpha_0$  and  $\alpha_1$  are constants depending on the geometry of the orotron. Substituting equation (5) into equation (4b), one obtains for the output power

$$P_{out} = \begin{cases} 0, & I_0 < \frac{G_0 + G_{out}}{\alpha_0}, \\ \frac{1}{I_0 \alpha_1} [I_0 \alpha_0 - (G_0 + G_{out})], & I_0 > \frac{G_0 + G_{out}}{\alpha_0}. \end{cases} \quad (6)$$

\*This follows from a power series expansion of the electron beam motion in the rf electric field.

Equation (6) may be written in terms of more familiar quantities. Identifying

$$I_t = \frac{G_0 + G_{out}}{\alpha_0}, \quad P_{max} = \frac{\alpha_0}{\alpha_1}, \quad (7)$$

one obtains

$$\frac{P_{out}}{P_{max}} = \begin{cases} 0, & I_0 < I_t, \\ \frac{I_0 - I_t}{I_0}, & I_0 > I_t. \end{cases} \quad (6')$$

Thus,  $I_t$  represents the threshold current (starting current) below which oscillation does not take place.  $P_{max}$  is the maximum power obtained from the oscillator by letting  $I_0 \rightarrow \infty$  in equation (6').

Equation (4a) states that the output radiation from the oscillator is monochromatic at frequency  $\omega_0$ . However, the presence of the noise source in figure 2 leads to a finite spectral width of the output and also modifies equation (6').

Consider the equivalent circuit in figure 2, where  $i(\omega)$  represents broadband noise. The noise may be parametrized by recalling\* that the Smith-Purcell radiation (which this noise represents) is proportional to the square of the electron beam current. Thus, the power dissipated by the resistive elements  $G_0$  and  $G_{out}$  (that is, without the resonant cavity and the feedback) is given by

$$\begin{aligned} p_n(\omega) d\omega &= \frac{1}{2} \frac{|i(\omega)|^2}{G_0 + G_{out}} d\omega \\ &= \frac{1}{2} I_0^2 r, d\omega, \end{aligned} \quad (8)$$

where  $p_n(\omega)$  is the spectral density of the noise, and  $r$ , is a parameter characterizing the Smith-Purcell radiation due to fluctuations in the electron beam. The voltage drop across the circuit in figure 2 at frequency  $\omega$  is given by

$$V(\omega) = \frac{i(\omega)}{G_0 + G_{out} - G_{beam} + iB_0(\omega - \omega_0)}, \quad (9)$$

\*O. A. Tret'yakov, S. S. Tret'yakov, and V. P. Shestopalov: *Radio Eng. Electron. Phys.*, 10 (1964), 1059.

and the spectral power density dissipated in the output conductance is

$$p_{out}(\omega) = \frac{1}{2} G_{out} |V(\omega)|^2 \quad (10)$$

$$= \frac{1}{2} \frac{G_{out} |i(\omega)|^2}{(G_0 + G_{out} - G_{beam})^2 + B_0^2 (\omega - \omega_0)^2}$$

The resonant cavity is characterized by its quality factor,  $Q$ , given by

$$Q = \frac{B_0 \omega_0}{2(G_0 + G_{out})} \quad (11)$$

and one may define an effective  $Q$ ,  $Q_{eff}$ , for the beam-cavity system by

$$Q_{eff} = \frac{B_0 \omega_0}{2(G_0 + G_{out} - G_{beam})} \quad (12)$$

Furthermore, the output coupling factor is defined as

$$\lambda = \frac{G_{out}}{G_{out} + G_0} \quad (13)$$

Using equations (11) to (13) and (8) in equation (10), one arrives at the spectral decomposition of the output power:

$$p_{out}(\omega) = \frac{\lambda I_0^2 r \omega_0^2}{8Q^2 \left[ (\omega - \omega_0)^2 + \left( \frac{\omega_0}{2Q_{eff}} \right)^2 \right]} \quad (14)$$

and the total power output is

$$P_{out} = \int p_{out}(\omega) d\omega$$

$$= \frac{\pi \lambda r \omega_0 I_0^2 Q_{eff}}{4Q^2} \quad (15)$$

Recalling that equation (12) defines  $Q_{eff}$  and that  $G_{beam}$  is dependent upon  $P_{out}$ , one sees that equation (15) must be solved self-consistently to obtain  $P_{out}$ . This solution necessitates stating a specific form for  $G_{beam}$ , as done in equation (5). However, equation (15) may be inverted to give the effective quality factor

$$Q_{eff} = \frac{4Q^2 P_{out}}{\pi \lambda r \omega_0 I_0^2} \quad (16)$$

whence one can get the line width\* of the output radiation from equation (14),

$$\delta_{1/2} = \frac{\omega_0}{2Q_{eff}} = \frac{\pi \lambda r \omega_0^2 I_0^2}{8Q^2 P_{out}} \quad (17)$$

This relation holds in general, independent of the specific functional form of  $G_{beam}$ .

To take a specific example,  $G_{beam}$  of the form given by equation (5), use of equation (7) in equation (12) leads to

$$Q_{eff} = \frac{Q}{1 - \frac{I_0}{I_1} \left( 1 - \frac{P_{out}}{P_{max}} \right)} \quad (18)$$

and therefore equation (16) becomes

$$\frac{Q}{1 - \frac{I_0}{I_1} \left( 1 - \frac{P_{out}}{P_{max}} \right)} = \frac{4Q^2 P_{out}}{\pi \lambda r \omega_0 I_0^2} \quad (19)$$

which is a quadratic equation in  $P_{out}$ . The solution is

$$P_{out} = \frac{P_{max}}{2} \left\{ 1 - \frac{I_1}{I_0} + \left[ \left( 1 - \frac{I_1}{I_0} \right)^2 + \frac{\pi \lambda r \omega_0 I_0^2 I_1}{P_{max} Q} \right]^{1/2} \right\} \quad (20)$$

\*Defined as the deviation of frequency from line center at which the spectral power density falls to half its maximum, that is, the half width of the line.

One then defines the parameter

$$P_n^{(0)} = \frac{\pi \lambda r \omega_0 I^2}{4Q} \quad (21)$$

The physical significance of  $P_n^{(0)}$  is that it is the output power that would be detected in the absence of feedback at  $I_0 = I$ . It is a measure of the noise power level in the system. Using equation (21), equation (20) becomes

$$P_{out} = \frac{P_{max}}{2} \left\{ 1 - \frac{I_0}{I_1} + \left[ \left( 1 - \frac{I_0}{I_1} \right)^2 + 4 \frac{I_0}{I_1} \frac{P_n^{(0)}}{P_{max}} \right]^{1/2} \right\} \quad (22)$$

Figure 3 shows the output characteristics of an orotron with  $P_n^{(0)}/P_{max} = 10^{-2}$  compared with those of an ideal oscillator. Because of the relative weakness of Smith-Purcell radiation, the ratio  $P_n^{(0)}/P_{max}$  is more likely to be  $\sim 10^{-6}$ ; thus, the orotron should behave as an ideal oscillator.

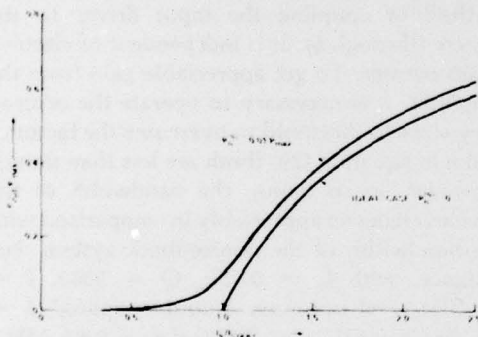


Figure 3. Power characteristics of orotron oscillation.

The line width of the oscillator output is given by equation (17); substituting equation (22) into equation (17), one gets

$$\delta_{1/2} = \frac{1}{2} \delta_{1/2}^{(0)} \left\{ \left[ \left( \frac{I_0}{I_1} - 1 \right)^2 + 4 \frac{I_0}{I_1} \frac{P_n^{(0)}}{P_{max}} \right]^{1/2} - \left( \frac{I_0}{I_1} - 1 \right) \right\} \quad (23)$$

where  $\delta_{1/2}^{(0)} = \omega_0/2Q$  is the line width of the passive resonator. Figure 4 shows the line width characteristics of an orotron with  $P_n^{(0)}/P_{max} = 10^{-2}$  compared with those of an ideal oscillator. Ideally, the line width should decrease from  $\delta_{1/2}^{(0)}$  in a linear fashion to zero at threshold and remain zero after threshold. However, the line width attains a minimum at  $I_0 = 1.5I_1$  and increases slowly with increasing current beyond that point. In fact, it can be shown from equation (23) that, if  $P_n^{(0)}/P_{max} \ll 1$ , there is a minimum at  $I_0 = 1.5I_1$  with a value

$$\delta_{1/2}^{min} = 6.75 \frac{P_n^{(0)}}{P_{max}} \delta_{1/2}^{(0)} \quad (24)$$

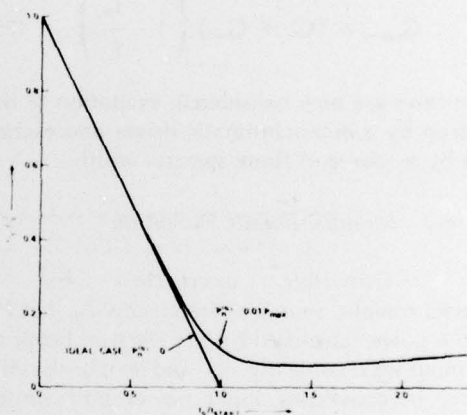


Figure 4. Line width characteristics of orotron oscillation.

The value  $P_n^{(0)}/P_{max} = 10^{-2}$  is used in figures 3 and 4 so that the salient features of the current dependence are clearly visible. A more likely value is  $10^{-6}$ . To choose a specific example, one may take  $P_{max} = 10$  W,  $P_n^{(0)} = 10$   $\mu$ W, and  $Q = 3000$ . At frequency  $f = 75$  GHz, equation (17) gives  $\delta_{1/2}^{(0)} = 12.5$  MHz. The minimum line width above threshold, from equation (24), is  $\delta_{1/2}^{min} = 84$  Hz. Thus, if the above conditions hold, the actual line width of the orotron oscillator above threshold is determined by the stability and the regulation of the orotron power supply (unpublished data), rather than by the inherent noise characteristics of the system.



#### 4. AMPLIFICATION CHARACTERISTICS

The orotron operates as an amplifier when the current source in the equivalent circuit (fig. 2) represents the effect of an external driver (fig. 1, input waveguide). The input signal is assumed to be large enough so that the noise may be ignored, yet small enough so that we may perform a small signal analysis of the equivalent circuit.

We consider the orotron operating below threshold.\* If the input signal is sufficiently weak, one may neglect the dependence of the beam conductance on power and simply write

$$G_{beam} = (G_0 + G_{out}) \left( 1 - \frac{I_0}{I_s} \right). \quad (25)$$

Two cases are now considered: excitation of the orotron by a monochromatic driver and excitation by a source of finite spectral width.

##### 4.1 Monochromatic Excitation

Consider excitation by a monochromatic source of frequency  $\omega_D$ . Let  $P_{in}$  be the power absorbed by the electron beam at the input waveguide (fig. 1), and let  $\eta$  be the efficiency in converting input power into Smith-Purcell radiation. The current,  $i(\omega_D)$ , may be related to  $P_{in}$  by considering the power dissipated in the load conductance,  $G_0 + G_{out}$ :

$$\frac{|i(\omega_D)|^2}{2(G_0 + G_{out})} = \eta P_{in}. \quad (26)$$

The output power is derived in the same manner as in section 3; the result is

$$P_{out} = \frac{\lambda \eta P_{in} \omega_0^2}{4Q^2 \left[ (\omega_D - \omega_0)^2 + \left( \frac{\omega_0}{2Q_{eff}} \right)^2 \right]} \quad (27)$$

\*In this region, the orotron operates as a linear amplifier. Above threshold, amplifier output power is no longer directly proportional to input power.

where  $Q_{eff} = Q_0[1 - I_0/I_s]^{-1}$ . When  $\omega_D = \omega_0$ ,

$$P_{out} = P_{in} \lambda \eta \left( \frac{Q_{eff}}{Q} \right)^2, \quad (28)$$

and so the power gain of the amplifier is

$$A_p = \lambda \eta \left( \frac{Q_{eff}}{Q} \right)^2. \quad (29)$$

From equation (27), the half bandwidth of the amplifier is

$$\delta_0 = \frac{\omega_0}{2Q_{eff}} = \delta_{1/2}^{(0)} \frac{Q}{Q_{eff}}, \quad (30)$$

and so the root gain-bandwidth product is

$$(A_p)^{1/2} \delta_0 = \frac{\omega_0}{2Q} (\lambda \eta)^{1/2}, \quad (31)$$

which depends only on the passive resonator properties (through  $\omega_0$ ,  $Q$ , and  $\lambda$ ) and the method of coupling the input driver to the system (through  $\eta$ ). It is independent of electron beam current. To get appreciable gain from the amplifier, it is necessary to operate the orotron very close to threshold to overcome the factors  $\lambda$  and  $\eta$  in equation (29) (both are less than unity). However, in so doing, the bandwidth of the device is reduced appreciably in comparison with the bandwidth of the nonfeedback system. For instance, with  $I_0 = 0.95I_s$ ,  $Q = 3000$ ,  $f = 75$  GHz, and optimum output coupling\*  $\lambda = 0.5$ , one gets  $Q_{eff} = 60,000$  and  $\delta_0 = 0.63$  MHz. If  $\eta = 0.1$  is chosen (a not unreasonable value), the gain is  $A_p = 20$ .

##### 4.2 Excitation by Source of Finite Spectral Width

If the driver is not monochromatic, one must perform an integral over frequency of a quantity similar to that given in equation (27) multiplied by the line shape of the driver to ob-

\*D. E. Wortman and R. P. Leavitt, *Near Millimeter Wave Orotion Research Study*, Harry Diamond Laboratories (October 1978) (draft).



tain the total power output. One may consider a source of Lorentzian line shape such that

$$\frac{|i(\omega)|^2}{2(G_0 + G_{mcr})} = \frac{\eta \delta_D P_{in}}{\pi[(\omega - \omega_D)^2 + \delta_D^2]}, \quad (32)$$

which is normalized so that the power dissipated in the load conductance,  $G_0 + G_{mcr}$ , is  $\eta P_{in}$ , as before. The quantity  $\delta_D$  is the driver line width. The spectral density of the output power is

$$P_{out} = \frac{\lambda \eta \delta_D \omega_0^2 P_{in}}{4\pi Q^2 [(\omega - \omega_D)^2 + \delta_D^2] [(\omega - \omega_0)^2 + \delta_0^2]}, \quad (33)$$

and the total output power is

$$P_{out} = \frac{\lambda \eta P_{in} \delta_0 Q_{off}^2}{Q^2} \frac{\delta_0 + \delta_D}{\Delta^2 + (\delta_0 + \delta_D)^2}, \quad (34)$$

where  $\Delta = \omega_D - \omega_0$ . For sufficiently small  $\delta_D$ , the output power of equation (34) approaches that of a monochromatic source as given by equation (27). Figures 5 to 10 depict the frequency spectrum of the output radiation for various values of  $\delta_D$ ,  $\delta_0$ , and  $\Delta$ . Also shown are the individual spectra of the driver and the amplifier. To accurately reproduce the spectral characteristics of the driver, the width of the orotron response must be much larger than the driver width. In fact, it can be shown from equation (33) that to first order in  $\delta_D^2$  the shape of the response curve is unchanged, but is shifted relative to the driver by an amount

$$|\Delta \omega_{out}| = -\Delta \frac{\delta_D^2}{\Delta^2 + \delta_0^2}. \quad (35)$$

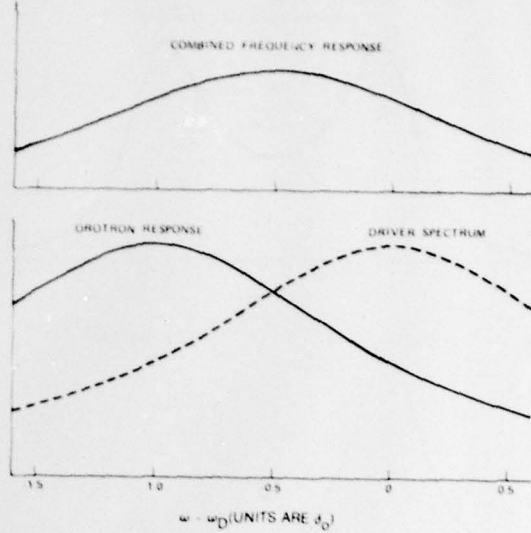


Figure 5. Orotion amplifier frequency response:  
 $\delta_D = \delta_0 = \Delta$ .

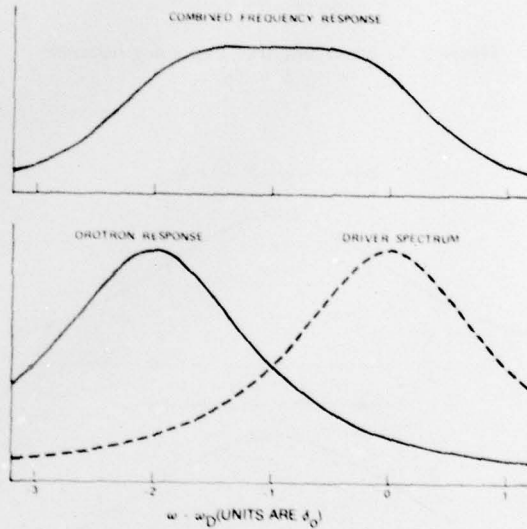


Figure 6. Orotion amplifier frequency response:  
 $\delta_D = \delta_0$ ,  $\Delta = 2\delta_0$ .

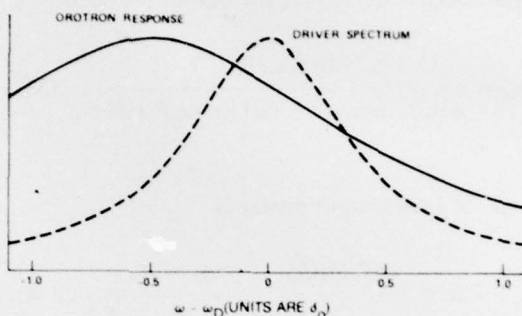
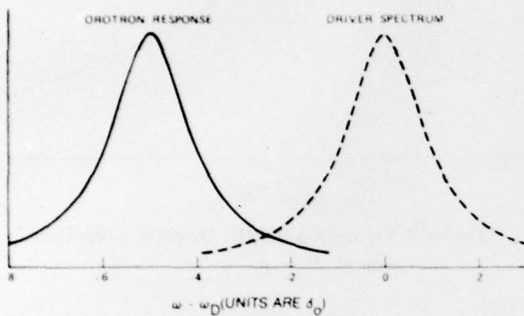
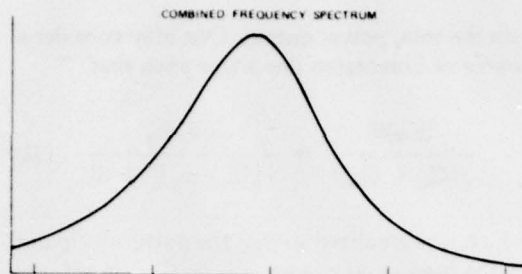
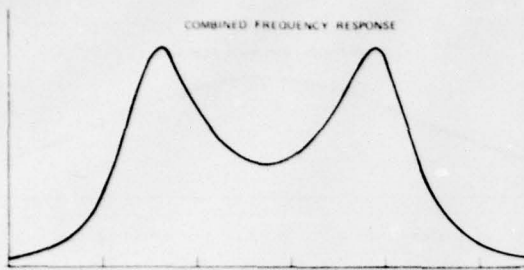


Figure 7. Orotion amplifier frequency response:  
 $\delta_D = \delta_0, \Delta = 5\delta_0.$

Figure 9. Orotion amplifier frequency response:  
 $\delta_D = 0.4\delta_0, \Delta = 0.5\delta_0.$

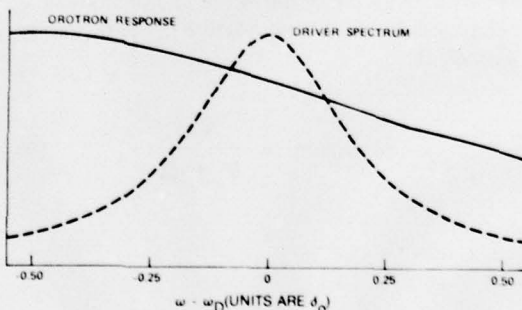
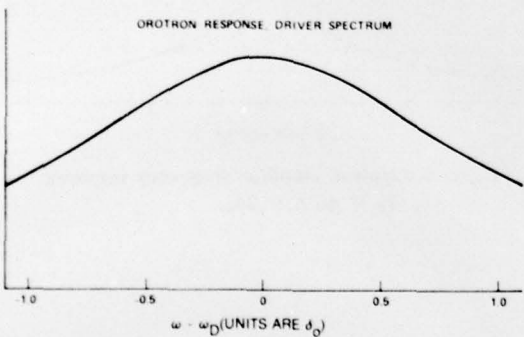
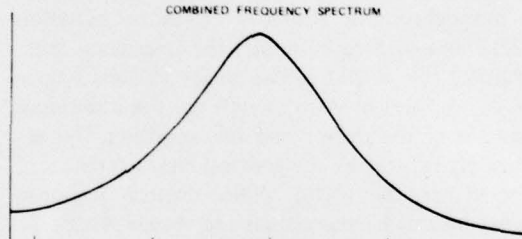
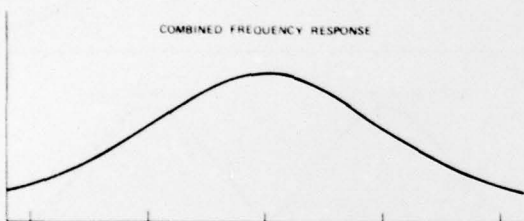


Figure 8. Orotion amplifier frequency response:  
 $\delta_D = \delta_0, \Delta = 0.$

Figure 10. Orotion amplifier frequency response:  
 $\delta_D = 0.2\delta_0, \Delta = 0.5\delta_0.$

## 5. CONCLUSIONS

The orotron operates as a nearly ideal oscillator if  $P_n^{(0)} \ll P_{max}$ , where  $P_n^{(0)}$  and  $P_{max}$  characterize, respectively, the noise level and the power output from the system. The line width of the output radiation above threshold is reduced by a factor of  $6.75 P_n^{(0)} / P_{max}$  relative to the line width of the passive open resonator. The dependence of output power and line width on electron beam current was determined. For reasonable signal-to-noise ratios, the calculated line width above threshold is so small that the actual line width of the system depends on the stability of the orotron power supply rather than the inherent noise characteristics of the orotron.

A small signal analysis (neglecting the power dependence of the electron beam conductance) has been performed to determine the amplification characteristics of the orotron. Below threshold, the orotron behaves as a linear amplifier with a gain that increases as the threshold current is approached. The product of the square root of the power gain and the half bandwidth is a constant, depending only on the

geometry of the system and not on the electron beam current. Amplification characteristics were determined when the orotron was excited by a source of finite spectral width. For the orotron to faithfully reproduce the spectral content of the input, the source width must be much less than the bandwidth of the orotron response.

The phenomenological parameters introduced in this report (that is,  $P_n^{(0)}$ ,  $I_t$ , and  $P_{max}$ ) are in principle calculable from the fundamental theory of orotron operation. In particular,  $P_n^{(0)}$  may be determined from the theory of Smith-Purcell radiation. The threshold current,  $I_t$ , is determined from the linear theory of electron bunching, and  $P_{max}$  can be obtained from a nonlinear bunching calculation. These calculations will be the subject of future reports.

## ACKNOWLEDGEMENT

The author thanks Donald E. Wortman, Clyde A. Morrison, and Nick Karayianis for participating in useful discussions on the subject of this report.

#### LITERATURE CITED

1. F. S. Rusin and G. D. Bogomolov, Soviet Patent No. 195557 (1965).
2. N. Tagushi and S. Ono, Report of Research Group on Electron Devices (March 1964).
3. V. P. Shestopalov, Diffraction Electronics, Khar'kov (1976) (Trans. U.S. Joint Publication Service, April 1978).
4. S. J. Smith and E. M. Purcell, Phys. Rev., 92 (1953), 1069.
5. A. Yariv in Quantum Electronics, 2nd ed., John Wiley and Sons, Inc., New York (1975), 300 ff.
6. O. A. Tret'yakov, S. S. Tret'yakov, and V. P. Shestopalov, Radio Eng. Electron. Phys., 10 (1964), 1059.



# DISTRIBUTION

ADMINISTRATOR  
DEFENSE DOCUMENTATION CENTER  
ATTN DCC-TCA (12 COPIES)  
CAMERON STATION  
ALEXANDRIA, VA 22314

COMMANDER  
US ARMY RSCH & STD GP (EUR)  
ATTN LTC JAMES M. KENNEDY, JR.  
CHIEF, PHYSICS & MATH BRANCH  
FPO NEW YORK 09510

COMMANDER  
US ARMY MATERIEL DEVELOPMENT &  
READINESS COMMAND  
ATTN DRXAM-TL, HQ TECH LIBRARY  
ATTN DRCDE, DIR FOR DEVEL & ENGR  
ATTN DRCMD-ST  
ATTN DRCBSI, DR. P. DICKERSON  
5001 EISENHOWER AVENUE  
ALEXANDRIA, VA 22333

COMMANDER  
US ARMY MISSILE & MUNITIONS  
CENTER & SCHOOL  
ATTN ATSK-CTD-F  
REDSTONE ARSENAL, AL 35809

DIRECTOR  
US ARMY MATERIEL SYSTEMS ANALYSIS  
ACTIVITY  
ATTN DRXSY-MP  
ABERDEEN PROVING GROUND, MD 21005

DIRECTOR  
US ARMY BALLISTIC LABORATORY  
ATTN DRDAR-TSB-S (STINFO)  
ATTN DRXBR, DIRECTOR  
ATTN DRXBR-TB, F. J. ALLEN  
ATTN DRDAR-BLB, R. MCGEE  
ATTN DRDAR-BL, H. REED  
ABERDEEN PROVING GROUND, MD 21005

TELEDYNE BROWN ENGINEERING  
ATTN MS-44, DR. MELVIN L. PRICE  
CUMMINGS RESEARCH PARK  
HUNTSVILLE, AL 35807

ENGINEER SOCIETIES LIBRARY  
345 EAST 47TH STREET  
NEW YORK, NY 10017

COMMANDER  
US AIR FORCE GEOPHYSICAL LAB  
ATTN DR. S. A. CLOUGH  
L. G. HANSCOMB FIELD  
BEDFORD, MA 01731

COMMANDER  
US AIR FORCE ROME AIR  
DEVELOPMENT CENTER  
ATTN RADC/ETEN,  
DR. E. ALTSHULER  
L. G. HANSCOMB FIELD  
BEDFORD, MA 01730

COMMANDER  
US ARMY ATMOSPHERIC  
SCIENCES LABORATORY  
ATTN DR. H. RACHELLE  
ATTN DRSEL-BL-AS-P,  
DR. K. WHITE  
ATTN DRSEL-BL, LIBRARY  
WHITE SANDS MISSILE RANGE, NM 88002

COMMANDER  
US ARMY ELECTRONICS COMMAND  
ATTN DRSEL-TL-IJ, DR. H. JACOBS  
ATTN DRSEL-TL-IJ, DR. A. KERECHAN  
ATTN DRSEL-CT-R, R. PEARCE  
ATTN DRSEL-CT-L, DR. R. ROHDE  
FT MONMOUTH, NJ 07703

DIRECTOR  
ELECTRONICS TECHNOLOGY &  
DEVICES LABORATORY  
ATTN DELET-B, MR. REINGOLD  
FT MONMOUTH, NJ 07703

COMMANDER  
US ARMY FOREIGN SCIENCE AND  
TECHNOLOGY CENTER  
220 SEVENTH STREET, NE  
ATTN DRXST-SD, DR. O. R. HARRIS  
CHARLOTTESVILLE, VA 22901

COMMANDER  
US ARMY MIRADCOM  
ATTN DRSMI-REO, DR. G. EMMONS  
ATTN DRDMI-TRO, DR. W. L. GAMBLE  
ATTN DRDMI-TRO, DR. B. D. GUENTHER  
ATTN DRDMI-TR, DR. R. L. HARTMAN  
ATTN DRDMI-TB, REDSTONE SCIENCE  
INFORMATION CENTER  
ATTN A. H. GREEN  
REDSTONE ARSENAL, AL 35809

COMMANDER  
US ARMY NIGHT VISION & ELECTRO-OPTICS  
LABORATORY  
ATTN W. EALY  
ATTN DELNV-VI, J. R. MOULTON  
ATTN DELNV-II, DR. R. SHURTZ  
ATTN LIBRARY  
ATTN DR. R. C. BUSER  
FT BELVOIR, VA 22060

DISTRIBUTION (Cont'd)

COMMANDER  
US ARMY RESEARCH OFFICE  
ATTN DRXDO-PH, DR. R. LONTZ  
ATTN DRXDO-PH, DR. C. BOGHOSIAN  
ATTN DR. J. SUTTLE  
RESEARCH TRIANGLE PARK  
DURHAM, NC 27709

COMMANDER  
NAVAL RESEARCH LABORATORY  
ATTN DR. V. L. GRANATSTEIN  
ATTN CODE 7111, DR. J. P. HOLLINGER  
ATTN CODE 7122.1, DR. K. SHIVANANDAN  
ATTN CODE 7110, B. YAPLEE  
ATTN DR. L. YOUNG  
WASHINGTON, DC 20375

COMMANDER  
NAVAL SURFACE WEAPONS CENTER  
ATTN F-34, J. J. TETI, JR.  
DAHLGREN, VA 22448

COMMANDER  
NAVAL SURFACE WEAPONS CENTER  
ATTN R-42, N. GRIFF  
ATTN R-43, A. KRALL  
ATTN F-46, R. E. JENSEN  
WHITE OAK, MD 20910

COMMANDER  
BALLISTIC MISSILE DEFENSE AGENCY  
ADVANCED TECHNOLOGY CENTER  
ATTN BMD-ATC-D, C. JOHNSON  
P.O. BOX 1500  
HUNTSVILLE, AL 35807

DEFENSE ADVANCED RESEARCH PROJECTS AGENCY  
ATTN TTO, DR. J. TEGNELIA  
ATTN STO, DR. S. ZAKANYCZ  
1400 WILSON BLVD  
ARLINGTON, VA 22209

NASA/GODDARD SPACE FLIGHT CENTER  
ATTN CODE 723, N. MCAVOY  
GREENBELT, MD 20771

NATIONAL BUREAU OF STANDARDS  
ATTN DR. K. M. EVENSON  
ATTN DR. R. PHELAN  
BOULDER, CO 80302

NATIONAL OCEANOGRAPHIC AND  
ATMOSPHERIC ADMINISTRATION  
ATTN DR. V. E. DERR  
ATTN LIBRARY, R-51 TECH REPORTS  
BOULDER, CO 80303

EMORY UNIVERSITY--PHYSICS DEPARTMENT  
ATTN S. PERKOWITZ  
ATLANTA, GA 30322

ENVIRONMENTAL RESEARCH  
INSTITUTE OF MICHIGAN  
ATTN M. BAIR  
ATTN DR. G. H. SUITS  
P.O. BOX 618  
ANN ARBOR, MI 48107

FORD-AERONUTRONIC  
ATTN DR. D. E. BURCH  
FORD ROAD  
NEWPORT, CA 92663

GEORGIA INSTITUTE OF TECHNOLOGY  
ENGINEERING EXPERIMENT STATION  
ATTN J. J. GALLAGHER  
ATTN DR. J. WILTSE  
ATLANTA, GA 30332

HONEYWELL CORPORATE RESEARCH CENTER  
ATTN DR. P. W. KRUSE  
10701 LYNDAL AVE, SOUTH  
BLOOMINGTON, MN 55420

INSTITUTE FOR DEFENSE ANALYSES  
ATTN DR. V. J. CORCORAN  
400 ARMY-NAVY DRIVE  
ARLINGTON, VA 22202

THE IVAN A. GETTING LAB  
THE AEROSPACE CORPORATION  
ATTN DR. E. J. DANIELEWICZ, JR.  
ATTN DR. T. S. HARTWICK  
ATTN DR. D. T. HODGES  
P.O. BOX 92957  
LOS ANGELES, CA 90009

LITTON INDUSTRIES, INC.  
ELECTRON TUBE DIVISION  
ATTN P. BAHR  
ATTN J. HULL  
ATTN J. MUNGER  
1035 WESTMINISTER DRIVE  
WILLIAMSPORT, PA 17701

MASS INSTITUTE OF TECHNOLOGY  
FRANCIS BITTER NATIONAL  
MAGNET LABORATORY  
ATTN K. J. BUTTON  
ATTN DR. R. J. TEMKIN  
170 ALBANY STREET  
CAMBRIDGE, MA 02139

MASS INSTITUTE OF TECHNOLOGY  
LINCOLN LABORATORY  
ATTN C. BLAKE  
ATTN H. R. FETTERMAN  
ATTN DR. D. TEMME  
P.O. BOX 73  
LEXINGTON, MA 02173

DISTRIBUTION (Cont'd)

NORTHROP CORPORTION  
DEFENSE SYSTEMS DIVISION  
ELECTRON TUBE SECTION  
ATTN G. DOEHLER  
ATTN O. DOEHLER  
ATTN R. ESPINOSA  
ATTN R. MOATES  
DES PLAINES, IL 60018

R&D ASSOCIATES  
ATTN DR. G. GORDON  
P.O. BOX 9695  
MARINA DEL REY, CA 90291

RAYTHEON COMPANY  
MICROWAVE AND POWER TUBE  
DIVISION  
ATTN L. CLAMPITT  
ATTN R. HARPER  
FOUNDRY AVENUE  
WALTHAM, MA 02154

STANFORD RESEARCH INSTITUTE  
ATTN J. WATJEN  
3980 EL CAMINO ROAD  
PALO ALTO, CA 94306

UNIVERSITY OF ILLINOIS  
DEPARTMENT OF ELECTRICAL  
ENGINEERING--EERL-200  
ATTN DR. P. D. COLEMAN  
ATTN DR. T. A. DETEMPLE  
URBANA, IL 61801

UNIVERSITY OF LOWELL NORTH CAMPUS  
DEPARTMENT OF PHYSICS AND APPLIED PHYSICS  
ATTN DR. D. KORFF  
ATTN DR. G. WALDMAN  
UNIVERSITY AVENUE  
LOWELL, MA 01854

VARIAN ASSOCIATES  
PALO ALTO MICROWAVE TUBE DIVISION  
ATTN H. JORY  
ATTN A. KARP  
ATTN E. LIEN  
611 HANSEN WAY  
PALO ALTO, CA 94303

US ARMY ELECTRONICS RESEARCH  
& DEVELOPMENT COMMAND  
ATTN DR. R. S. WISEMAN, DRDEL-CT  
ATTN DR. J. SCALES, DRDEL-AP-CCM  
ATTN DR D. GIGLIO, DRDEL-AP-CCM  
ATTN DR. B. ZARWYN, DRDEL-AP-OA

HARRY DIAMOND LABORATORIES  
ATTN 00100, CDR/TECH DIR/TSO  
ATTN CHIEF, DIV 10000  
ATTN CHIEF, DIV 20000  
ATTN CHIEF, DIV 30000  
ATTN CHIEF, DIV 40000  
ATTN RECORD COPY, 94100  
ATTN HDL LIBRARY, 41000 (3 COPIES)  
ATTN HDL LIBRARY, 41000 (WOODBIDGE)  
ATTN CHAIRMAN, EDITORIAL COMMITTEE  
ATTN TECHNICAL REPORTS BRANCH, 41300  
ATTN H. DROPKIN, 11100  
ATTN H. GERLACH, 11100  
ATTN J. NEMARICH, 11300  
ATTN D. SCHAUBERT, 11500  
ATTN F. CROWNE, 13200  
ATTN R. LEAVITT, 13200 (3 COPIES)  
ATTN C. MORRISON, 13200  
ATTN J. SATTTLER, 13200  
ATTN G. SIMONIS, 13200  
ATTN M. TOBIN, 13200  
ATTN T. WORCHESKY, 13200  
ATTN D. WORTMAN, 13200  
ATTN D. BARR, 13500  
ATTN T. LISS, 15300  
ATTN E. BROWN, 15400  
ATTN S. KULPA, 15400  
ATTN C. WILLETT, 15400  
ATTN H. BRANDT, 22300  
ATTN A. BROMBORSKY, 22300  
ATTN J. SOLN, 22300  
ATTN J. SILVERSTEIN, 22900  
ATTN M. SOKOLOSKI, 00210  
ATTN Q. KAISER, 13500  
ATTN G. A. HUTTLIN, 22900  
ATTN H. GIBSON, 13000